# Photon-Counting Computed Tomography – Basic Principles, Potenzial Benefits, and Initial Clinical Experience

## Photon-Counting-Computertomografie – Grundlagen, mögliche Vorteile und erste klinische Erfahrungen

Authors

Thomas Stein[1], Alexander Rau[1], Maximilian Frederik Russe[1], Philipp Arnold[1], Sebastian Faby[2], Stefan Ulzheimer[2], Meike Weis[3], Matthias F. Froelich[3], Daniel Overhoff[3], Marius Horger[4], Florian Hagen[4], Malte Bongers[4], Konstantin Nikolaou[4], Stefan O. Schönberg[3], Fabian Bamberg[1], Jakob Weiß[1]

Affiliations

1 Department of Diagnostic and Interventional Radiology, Medical Center-University of Freiburg, Germany
2 Computed Tomography, Siemens Healthcare GmbH, Forchheim, Germany
3 Department of Radiology and Nuclear Medicine, University Medical Centre Mannheim, Germany
4 Department of Radiology, University Hospitals Tübingen, Germany

Key words

Photon Counting, Computed Tomography, Diagnostic Imaging, Spectral Computed Tomography, Photon-Counting Detector, Energy-Integrating Detectors

**received** 29.08.2022
**accepted** 18.01.2023
**published online** 02.03.2023

Bibliography

Fortschr Röntgenstr 2023; 195: 691–698
**DOI** 10.1055/a-2018-3396
**ISSN** 1438-9029

Georg Thieme Verlag KG, Rüdigerstraße 14, 70469 Stuttgart, Germany

Correspondence

Thomas Stein
Department of Diagnostic and Interventional Radiology, Universitätsklinikum Freiburg Klinik für Radiologie, Hugstetter Str. 55, 79106 79111 Freiburg, Germany
Tel.: +49/7 61/27 03 94 40
thomas.stein@uniklinik-freiburg.de

### ABSTRACT

**Background** Photon-counting computed tomography (PCCT) is a promising new technology with the potential to fundamentally change today's workflows in the daily routine and to provide new quantitative imaging information to improve clinical decision-making and patient management.

**Method** The content of this review is based on an unrestricted literature search on PubMed and Google Scholar using the search terms "Photon-Counting CT", "Photon-Counting detector", "spectral CT", "Computed Tomography" as well as on the authors' experience.

**Results** The fundamental difference with respect to the currently established energy-integrating CT detectors is that PCCT allows counting of every single photon at the detector level. Based on the identified literature, PCCT phantom measurements and initial clinical studies have demonstrated that the new technology allows improved spatial resolution, reduced image noise, and new possibilities for advanced quantitative image postprocessing.

**Conclusion** For clinical practice, the potential benefits include fewer beam hardening artifacts, radiation dose reduction, and the use of new contrast agents. In this review, we will discuss basic technical principles and potential clinical benefits and demonstrate first clinical use cases.

### Key Points:

- Photon-counting computed tomography (PCCT) has been implemented in the clinical routine
- Compared to energy-integrating detector CT, PCCT allows the reduction of electronic image noise
- PCCT provides increased spatial resolution and a higher contrast-to-noise ratio
- The novel detector technology allows the quantification of spectral information

### Citation Format

- Stein T, Rau A, Russe MF et al. Photon-Counting Computed Tomography – Basic Principles, Potenzial Benefits, and Initial Clinical Experience. Fortschr Röntgenstr 2023; 195: 691–698

### ZUSAMMENFASSUNG

**Hintergrund** Die Technologie der Photonen zählenden Computertomografie hat Einzug in die klinische Praxis gehalten und wird erstmals in der klinischen Routine eingesetzt. Während die ersten Erfahrungen mit diesem Verfahren in bestimmten Patientengruppen gemacht werden, hat die Technologie das Potenzial, bestehende Arbeitsabläufe zu verändern und öffnet neue Möglichkeiten in der diagnostischen Bildgebung.

**Methode** Der Inhalt dieser Übersicht basiert auf einer uneingeschränkten Literaturrecherche in den Datenbanken PubMed

und Google Scholar unter der Verwendung der Suchbegriffe “Photon-Counting CT”, “Photon-Counting detector”, “spectral CT”, “Computed Tomography” sowie auf den Erfahrungen der Autoren.

**Ergebnisse** Der grundlegende Unterschied zu den derzeit etablierten energieintegrierenden CT-Detektoren besteht darin, dass die PCCT die Zählung jedes einzelnen Photons auf Detektorebene ermöglicht. Basierend auf der identifizierten Literatur haben PCCT-Phantommessungen und erste klinische Studien gezeigt, dass die neue Technologie eine verbesserte räumliche Auflösung, eine reduziertes Bildrauschen und neue Möglichkeiten für neue quantitative Bildnachbearbeitung ermöglicht.

**Schlussfolgerung** PCCT ist eine neuartige, innovative Technologie mit dem Potenzial, viele der derzeitigen Einschränkungen der CT-Bildgebung in der klinischen Praxis zu überwinden. In diesem Review diskutieren wir grundlegende technische Prinzipien, potenzielle klinische Vorteile und demonstrieren erste klinische Anwendungsfälle.

**Kernaussagen**

- Die Photon-Counting-Computertomografie (PCCT) wird erstmals in der klinischen Routine eingesetzt
- Verglichen mit herkömmlichen CT ermöglicht die PCCT eine Reduzierung des elektronischen Bildrauschens
- PCCT bietet eine höhere räumliche Auflösung und ein besseres Kontrast-Rausch-Verhältnis
- Die neuartige Detektortechnologie ermöglicht die Quantifizierung von spektralen Bildinformationen

## Introduction

Photon-counting computed tomography (PCCT) was launched in the clinical routine in July 2021 and has the potential to fundamentally change today’s workflows. This article summarizes the technical principles and potential clinical benefits of the new photon-counting detector (PCD) technology in comparison to the currently established energy-integrating detectors (EID) and presents initial experiences from daily practice.

Since its clinical introduction in the 1970 s, computed tomography has revolutionized diagnostic workflows and patient management [1]. The developments from the early beginnings to current clinical practice were only possible due to major innovations such as the development of spiral CT and multi-slice systems with a higher pitch, as well as the acquisition of dual energy (DE) data at a comparable radiation dose to that of single-source CT systems. This has significantly expanded the range of indications to include vascular, cardiac, and functional imaging [2–5].

However, a noteworthy disadvantage of these EID systems can be attributed to the fact that the energy of the X-ray photons is measured indirectly using a scintillator that transforms incoming X-ray photons into visible light before the signal is converted into an electrical current (▶ **Fig. 1a**). Moreover, the detected signal is a cumulative measure of the energy of all incoming X-ray photons and does not contain information about their absolute number and individual energy level.

The photon-counting technology, which has been developed over the last two decades, has the potential to overcome these limitations by solving several physical challenges, such as signal splitting at the borders of the detector pixels, energy loss of X-rays due to K-escape, and the so-called “pulse pile-up”, where the high photon flux density commonly seen in medical CT can cause overlapping low-energy pulses to be falsely registered as high-energy hits [6, 7]. After successful implementation in preclinical scanners, photon-counting detector CT has now entered the clinical routine and reduces the limitations of energy-integrating CT as elucidated in the remainder of this review. While the first clinical system was introduced by Siemens Healthineers in late 2021, other major vendors such as Philips, GE, and Canon are expected to enter the market with clinical photon-counting CT systems soon.

## Photon-counting detector – technical background

Current EID CT relies on solid-state scintillation detectors consisting of a scintillator with septa and a photodiode array. Detector cells have a width of about 0.25–0.625 mm, projected to the CT’s isocenter [8]. Incoming X-ray photons generate a shower of visible light within the scintillator, which is subsequently converted into an electric signal by the photodiode. Here, the detected signal is proportional to the total energy of all photons during a measurement interval, without specific information about an individual photon or its energy. The septa in the scintillator material are necessary to partition the different detector elements. This prevents light photons from crossing between the detector elements. However, they limit the geometric dose efficiency, especially when trying to build smaller scintillator detector elements as depicted in ▶ **Fig. 2a, b** [9, 10].

Most PCDs for clinical and preclinical use are composed of semiconductors such as cadmium telluride (CdTe), cadmium zinc telluride (CdZnTe), and silicon [11]. The semiconductor layer is located between a cathode and a pixelated anode, across which a high voltage of about 800–1000 V is applied [12]. As shown in ▶ **Fig. 1b,** PCDs convert each incoming X-ray photon directly into electrical signals by generating a charge cloud of electron-hole pairs. The resulting charge clouds induce current pulses where the height of the pulses is proportional to the energy of the incoming X-ray photons. The pulses are then individually counted as soon as they exceed a threshold and can thus be separated by energy thresholds.

Both, the intensity of the scintillation light and the resulting amplitude of the induced current pulse are proportional to the energy of the absorbed X-ray photons. All registered current pulses are integrated over the measurement time for a single projection. One of the major limitations of this approach is that low-energy X-ray photons, which carry most of the low contrast infor-

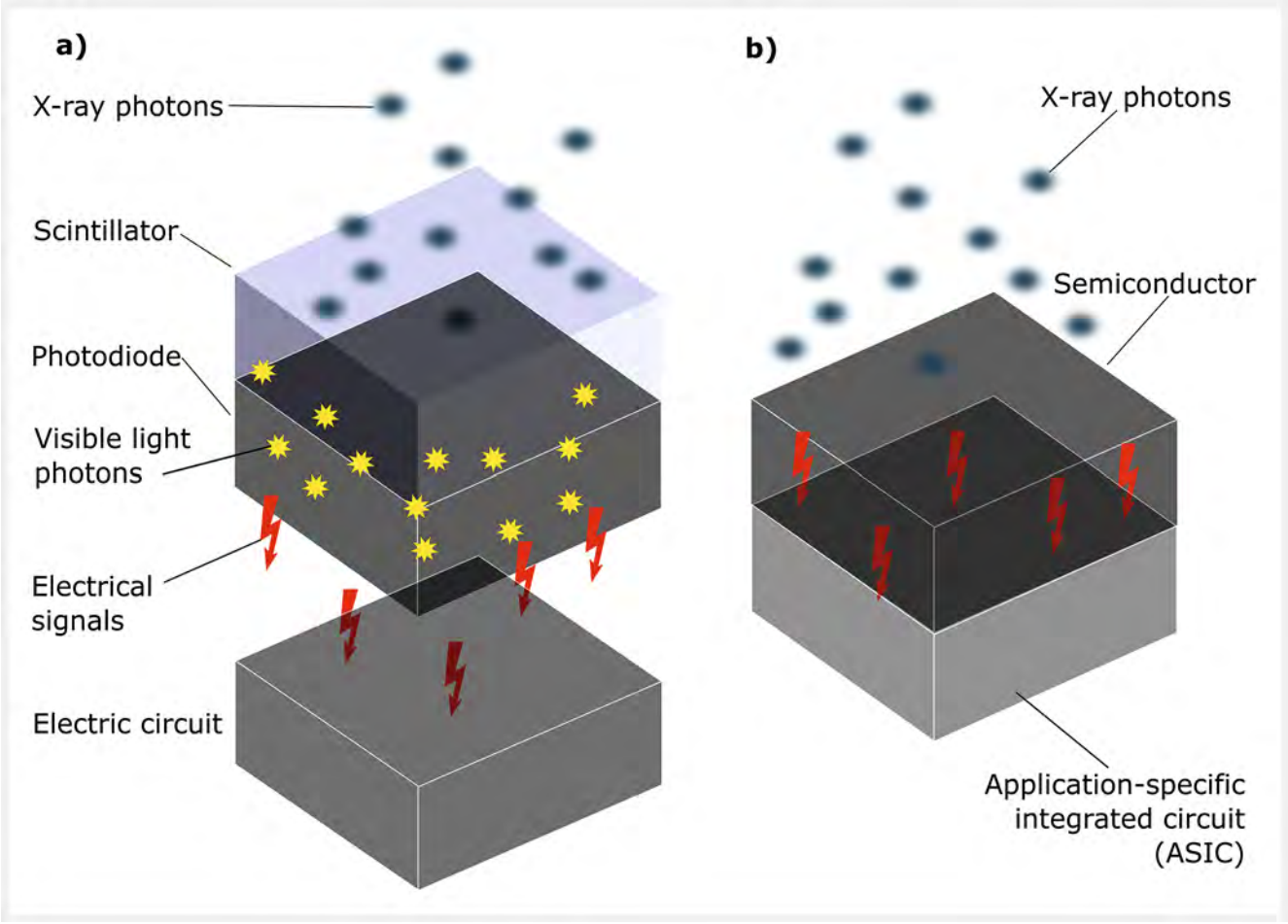


▶ **Fig. 1** **a** Energy-integrating scintillation detector. Individual detector cells made of a scintillator such as gadolinium oxide or gadolinium oxysulfide (GOS) absorb the X-ray photons and convert their energy into visible light. Subsequently, this light is detected by photodiodes placed on the back of each detector cell and converted into electric current. The detected signal is proportional to the cumulative photon energy without the ability to differentiate between individual photons. **b** In a PCCT detector, a semiconductor such as cadmium telluride absorbs the X-ray photons. This creates electron-hole pairs in a number proportional to the detected photon energy, which are separated into a strong electric field, resulting in a direct conversion of the detected signal into electric current. With this approach, individual photons can be counted and their respective energy can be measured.

mation, contribute significantly less to the integrated detector signal than higher-energy X-ray photons. This energy weighting substantially reduces the contrast-to-noise ratio (CNR) [13].

The new detector technology is also accompanied by physical challenges, such as k-escape, Compton scattering, pulse pile-up, and charge sharing, which must be noted. When X-ray photons arrive in the detector cell, secondary charge clouds can be created in addition to the primary charge clouds created due to the X-ray fluorescence of the detector material. When X-ray photons interact with the detector material, Compton scattering can result in only a portion of the primary energy being deposited as a charge cloud in the detector element. The remaining energy of the scattered photon can then reach another detector element. Charge sharing is when a charge cloud is created near a boundary of two pixel electrodes. As a result, this charge cloud can be measured by several neighboring pixel electrodes. If two pulses are generated almost simultaneously, the electrical pulses overlap, and this is called "pulse pile-up". In this case, incoming pulses are registered as a single pulse, which in turn leads to an inaccuracy in the measured photon energy.

## Improvement of spatial resolution

The spatial resolution of a CT detector is primarily determined by the size of the detector elements, which usually range between $0.8 \times 0.8\ mm^2$ to $1 \times 1\ mm^2$ at the detector level [14–17]. Increasing spatial resolution of EIDs beyond this point is limited due to the septa needed to prevent crosstalk between neighboring photodiodes and the reduced quantum efficiency of the detector, because X-ray photons absorbed in the separating layers do not contribute to the measured signal (▶ **Fig. 2a, b**) [15].

As shown in ▶ **Fig. 2c,** PCDs, on the other hand, come with smaller pixel sizes as they do not require separating layers between the detector pixels. Detector elements in PCCT range from $0.11 \times 0.11\ mm^2$ to $0.5 \times 0.5\ mm^2$. Including a geometric magnification factor, this results in a spatial resolution of $0.07 \times 0.07\ mm^2$ to $0.28 \times 0.28\ mm^2$ [14, 18–21]. In the standard multi-energy mode, PCD array subpixels are grouped and read out with the corresponding energy thresholds. In addition, the spatial resolution

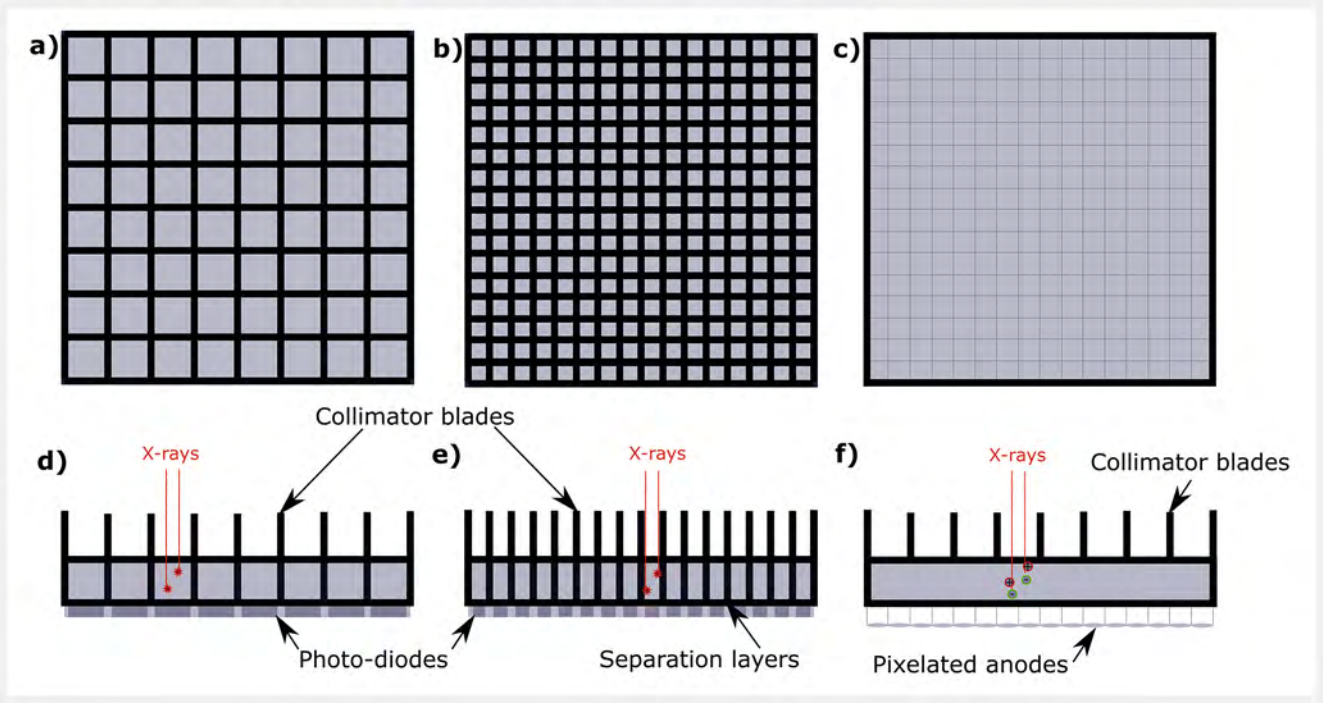


▶ **Fig. 2** **a, b** Schematic drawing of a scintillation detector in top view. Thin septa separate the detector elements. **b** While reducing the size of detector elements, the dead space relatively increases due to the overall larger area of the septa resulting in a decreased dose efficiency of the detector. **c** Schematic drawing of a PCD in top view. **d** & **e** Side view of EID. The individual detector elements are separated by light-reflecting septa. **f** Side view of PCD. The detector pixels are formed by the pixelated anodes without using additional separating layers. Collimator blades are still necessary to suppress scatter radiation.

can be increased by reading out individual subpixels in the special ultra-high resolution (UHR) mode.

Increased spatial resolution is of particular importance if subtle changes and small anatomical structures need to be evaluated such as in chest, bone, and cardiac CT where clinical benefits have been demonstrated by several preclinical and clinical investigators already [22–25]. In ▶ **Fig. 3**, we provide a representative clinical case of a 73-year-old patient who underwent cardiac CT to rule out significant coronary artery stenosis.

▶ **Fig. 4** shows another example of a patient with otosclerosis, which is a slowly progressing focal disorder of the bone metabolism of the otic capsule. In earlier stages, this leads to demineralization and spongiotic remodeling. Typical radiologic features comprise areas of increased bony radiolucency (usually at the fissula ante fenestram), but also widening of the oval window, thickening of the stapes, and a low-density demineralized zone outlining the cochlea (the so-called double ring sign) [26]. While the specificity of a high-resolution EID CT is high (around 95 %), its sensitivity is relatively low with approximately 58 %. In particular, submillimetric, retrofenestral, and dense sclerotic lesions are difficult to detect on conventional EID CT [27]. However, this can be of particular importance, as it is associated with sensorineural hearing loss and is treated with a cochlear implant rather than stapedectomy [28].

Image examples of PCCT and EID CT are given in ▶ **Fig. 4**. Delineation of the fenestral bony radiolucency is superior on PCCT images. In addition, the stapes implant (▶ **Fig. 4c**) is more sharply defined on PCCT with fewer artifacts compared to EID CT (▶ **Fig. 4f**). Finally, despite the gain in resolution, the total radiation dose was considerably lower for PCCT compared to EID CT (CTDIvol 16.6 mGy vs. 34.05 mGy).

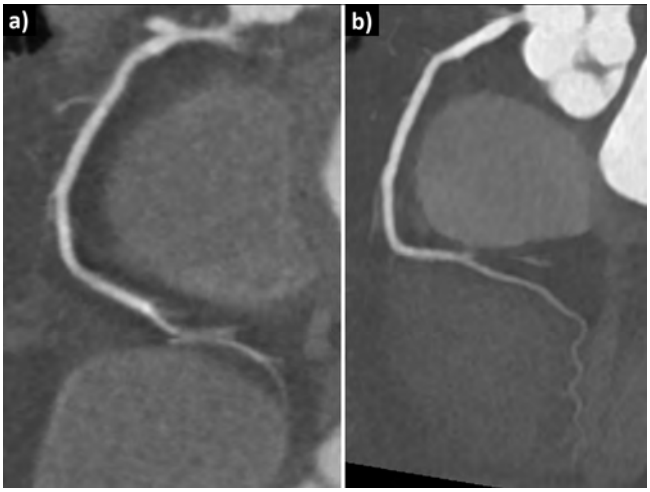


▶ **Fig. 3** Cardiac CT angiography of a 73-year-old patient. **a** depicts a curved multiplanar reconstruction of the RCA obtained on a second-generation EID dual-energy CT system, **b** depicts the same vessel acquired using a PC-CT system, which clearly shows the increased resolution and improved image quality compared to the EID detector.

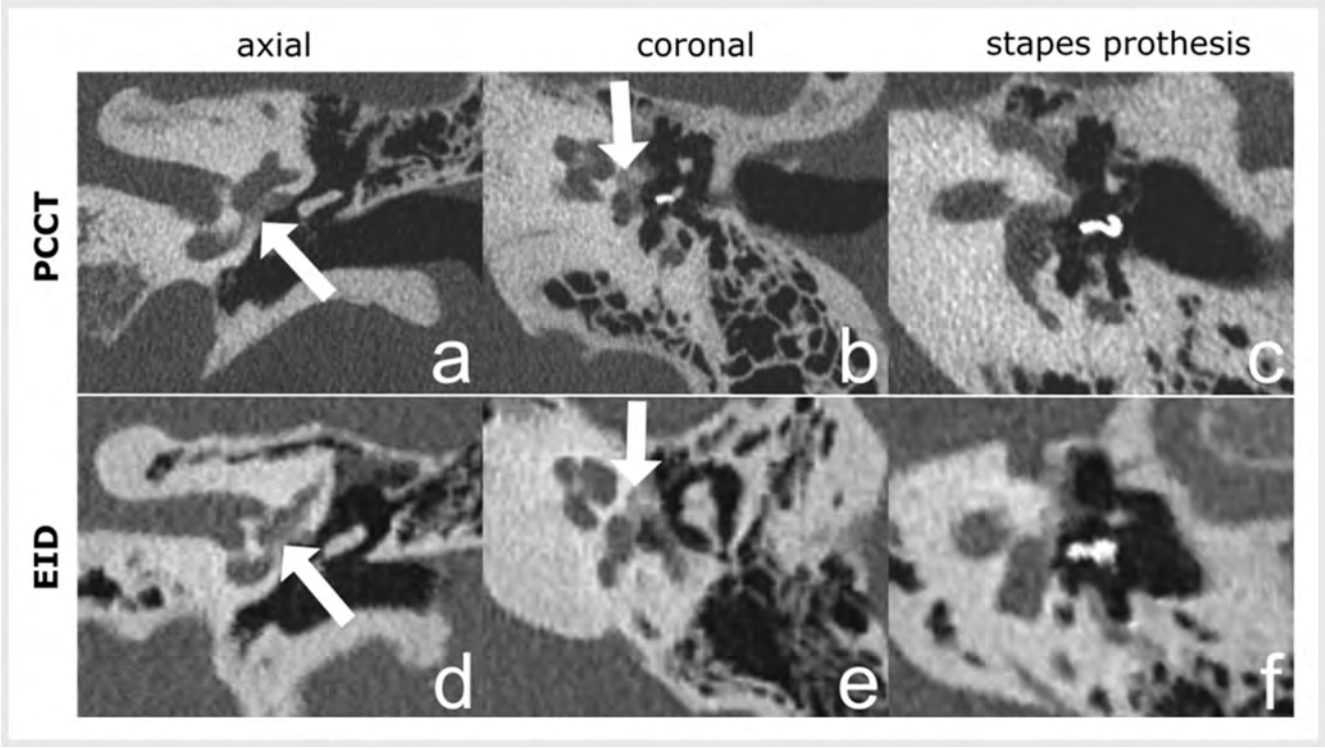


▶ **Fig. 4** Left temporal bone in two patients with fenestral otosclerosis, scanned with PCCT (NAEOTOM Alpha, Siemens Healthineers, Forchheim, Germany) (**a–c**, patient A) and conventional high-resolution EID CT (SOMATOM Definition Flash, Siemens Healthineers, Forchheim, Germany) (**d–f**, patient B). The bony lucencies adjacent to the oval window are clearly better differentiated from background noise in (**a**, coronary) and (**b**, axial) than in (**d**, coronary) and (**e**, axial). In addition, replacement prostheses are more sharply distinguishable in (**c**) than in (**f**).

## Electronic noise

Apart from spatial resolution, image quality is limited by electronic noise in EID CT. Noise in CT imaging is a composite of quantum noise and electronic noise. The quantum noise is affected by the number of photons, whereas the electronic noise results from the electronic circuitry in the system. As mentioned above, an EID measures the total X-ray energy detected during the time interval of a single projection, which includes the electronic noise as a random additive term in the measurement. At high doses, electronic noise is negligible as the quantum noise is proportional to the incident fluence rate, which in turn increases at high doses [29, 30]. Conversely, in situations with extremely low radiation doses or in extremely obese patients, the electronic noise level in EID CT scans will become comparable in strength to the low detector signal from the X-ray photons, resulting in noise streaks or drift in Hounsfield Unit stability [29].

Electronic noise usually has a constant low amplitude. Thus, when detected by a PCD, it can be interpreted as a photon with an energy at the lower end of the typical X-ray spectrum as shown in ▶ **Fig. 5**. This makes it possible to set a threshold and specifically exclude electronic noise from further signal processing and image reconstruction [31]. However, electronic noise may still have some minor effect on the detected signal as it artificially increases the energy of the detected photon by increasing its respective amplitude. Nevertheless, the elimination of electronic noise using a PCD provides more consistent image quality as shown in ▶ **Fig. 3** and noticeably reduces streak artifacts in comparison to EID [32]. Overall, this reduces image noise, improves the diagnostic quality of the acquired data and improves Hounsfield Unit stability [33]. PCCT may therefore allow new low-dose imaging protocols as electronic noise is currently the limiting factor with state-of-the-art EID scanners, and might thus be applied to pediatric imaging or lung cancer screening [22, 34].

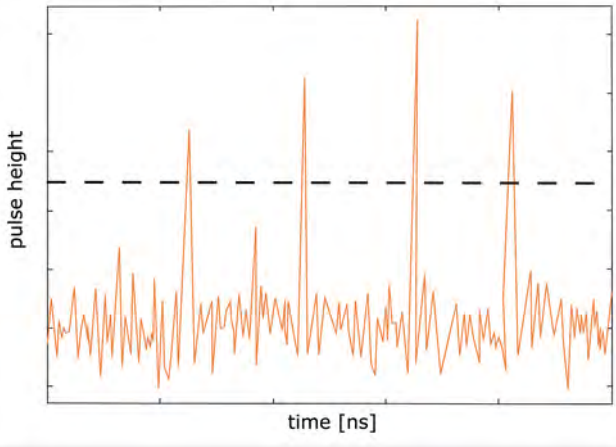


▶ **Fig. 5** In a PCD, voltage pulses are induced by the absorbed X-ray photons. These voltage pulses are counted as soon as they exceed a threshold value (dashed line). The pulse height corresponds to the energy of the incoming photons by direct conversion. Pulses with a low amplitude are counted as baseline noise which is caused for example by electronic noise.

## Artifact reduction

Metal artifacts are one of the strongest artifacts encountered in CT. These artifacts have a characteristic appearance and are caused by various physical processes, such as photon scattering, photon starvation, and beam hardening. In beam hardening, the effective photon energy of the X-ray beam, which contains a broad spectrum of energies, is shifted to the higher end of the spectrum after passing through the scanned object. These artifacts can have a massive impact on image quality and diagnostic confidence, and can drastically obscure critical structures of interest. Because PCCT sorts each photon by its energy, monoenergetic images at high keV levels can be reconstructed from the multispectral dataset, which allows for a significant reduction in beam hardening artifacts compared to EID [35]. In addition, the increase in spatial resolution also improves the reduction of partial volume effects, and thus further reduces artifacts, which might improve the assessment of small structures with high density such as coronary plaques [24].

The following case of an 85-year-old female patient who received occipito-vertebral fusion due to an atlas fracture demonstrates this in a typical clinical setting. A postoperative EID CT examination revealed bilateral resorption margins around the pedicular screws in C5. However, assessment was impaired due to metal artifact superimposition. After treatment of delayed wound healing, follow-up CT imaging of the cervical spine was performed on a PCCT after interim external immobilization of the neck.

Image examples of the two examinations are shown in ▶ **Fig. 6**. The clinically established standard is given for EID CT. The PCCT protocol was designed to mimic the current standard. In addition, inline calculation of virtual monoenergetic images at 130 keV was performed exploiting the multispectral data to improve assessment of the metallic implant and surrounding structures. The PCCT images provide superior image quality and improved assessment of the screw loosening as well as of adjacent osseous and soft tissue structures at a substantially reduced radiation dose (CTDIvol 12.45 mGy vs. 7.54 mGy).

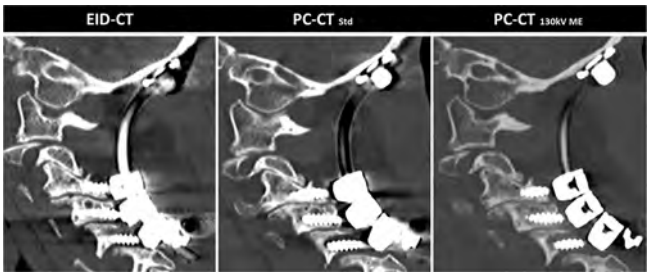


▶ **Fig. 6** Image example of an 85-year-old patient with posttraumatic cervical spinal fusion. The loosening of the right pedicle screw in C5 is most obvious in PCCT130keV whereas artifacts are strongest on EID CT. The radiation dose was substantially lower in the PCCT examination (CTDIvol 12.45 mGy vs. 7.54 mGy).

## Material decomposition

Spectral CT data is acquired by energy separation in PCCT. This data can be reconstructed in different energy ranges, or the energy information can be used for quantitative image analysis by energy weighting or material decomposition. In energy weighting, more weight is assigned to a particular energy bin relative to other energy bins [13, 33, 36, 37]. For material decomposition the full energy dependency of the attenuation curve in each image voxel needs to be identified [38, 39]. The underlying hypothesis that any material composed of light elements, such as human tissue, will have X-ray attenuation properties roughly equivalent to a combination of two base materials is represented by two bins [39]. Theoretically, any pair of materials can be chosen as base materials. However, in humans, a combination of water and calcium is assumed. As shown in ▶ **Fig. 7a**, this allows modelling of each human tissue in a diagram in which the axes represent the concentrations of the two base materials. Additional dimensions can be added using the element-specific K-edge for high atomic number elements, where a step-like change in attenuation occurs at a specific X-ray energy (▶ **Fig. 7b**). This allows the calculation of virtual monochromatic images, but also the distribution of a certain material in the body, as well as virtual non-contrast images [40] or material-specific color overlay images [40–42].

Furthermore, this approach can be employed for the quantification and separation of contrast agents. Symons et al. [41] were also able to show that the injection of different contrast agents at different time points can visualize the incorporation of the contrast agents in only one scan in the form of a multiphase image. This opens further possibilities, especially with regard to dose reduction, contrast agent reduction, and tissue characterization. Improving spectral imaging is also expected to improve the detectability of new contrast agents, especially k-edge contrast agents [43]. In addition to the currently approved contrast agents with iodine and gadolinium, further contrast agents are required to generate multiphase images, which can also be based on nanoparticles. However, more research is needed to pave the way to clinical practice and to investigate the true benefits with respect to improving patient care. The amount of contrast agent in an image voxel can be separated from the other components if three parameters are measured: the concentrations of water, calcium, and the contrast agent. To determine these three variables, measurements in three or more energy ranges are required [38] as shown in ▶ **Fig. 7b**. Existing methods for measuring iodine concentration at two energies must therefore rely on a priori assumptions about tissue composition. PCCT introduces the potential for more accurate measurements [6]. For example, iodine exhibits the K-edge at 33 keV. In order to perform independent quantification of iodine, it is necessary for photons to be transmitted at these low energies. This seems realistic for objects or patients with small diameters such as children [41, 42, 44, 45].

## Data storage and postprocessing

Due to the improved spatial resolution and new possibilities for quantitative image postprocessing, PCCT will substantially increase the amount of acquired data. Especially when working with larger matrices like 1024 × 1024 in combination with multi-

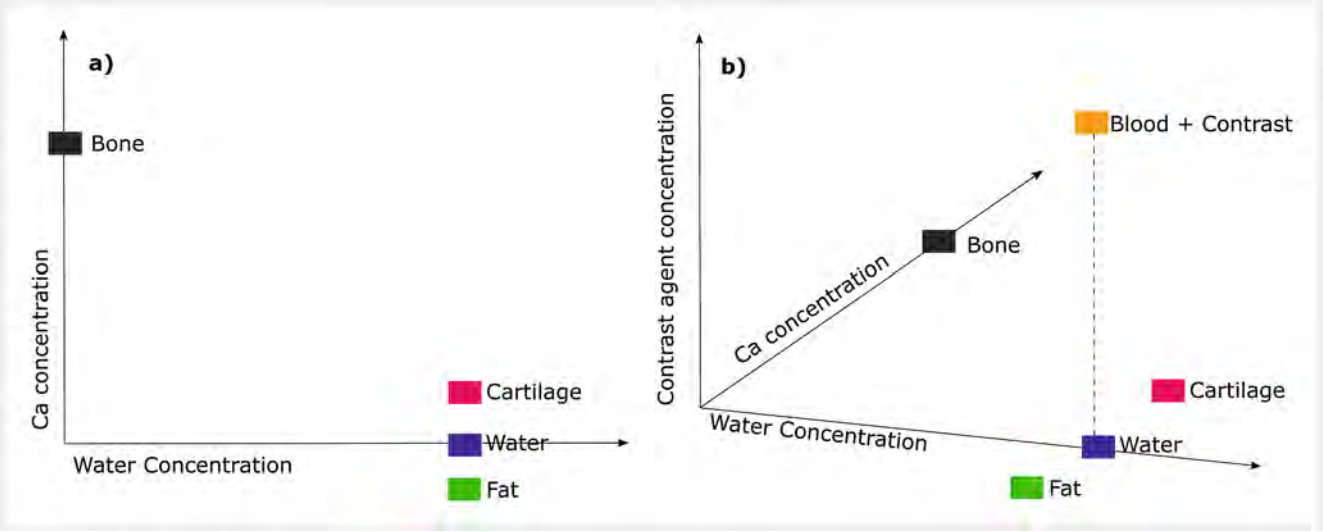


▶ **Fig. 7** Material decomposition. **a** The X-ray attenuation properties of any material in the human body correspond to a point in a two-dimensional diagram with water and calcium ($Ca^{2+}$) concentrations on the axes. **b** Including other K-edges extends the diagram into more dimensions (three shown here). This makes it possible to measure the contrast agent concentration independently of the calcium-water concentration.

spectral photon-counting CT data, the amount of data increases significantly. For example, reducing the slice thickness by 50 % and doubling the in-plane matrix increases data size by eight-fold per reconstruction method. As a result, datasets of a single patient/examination are likely to regularly exceed 10 gigabytes especially when exploiting the entire multispectral data for advanced postprocessing, such as calculating virtual monochromatic, virtual non-contrast, or virtual non-calcium images or performing different material decompositions. Therefore, new solutions for data handling, transfer, storage, and presentation as well as new algorithms for processing and analyzing data are required. With recent advances in artificial intelligence, new approaches for automated high-throughput data management and analysis will become available. Implementing such methods into clinical workflows has the potential to support and accelerate the clinical potential of PCCT in daily practice. Besides commercial solutions provided by all major vendors, several open-source tools like 3 D Slicer [46] or pyradiomics [47] are available for image analysis and are established in the research community. More recently developed solutions, such as JIP (DKFZ German cancer consortium, Heidelberg, Germany) and NORA (NORA Medical Imaging Platform Project, University Medical Center Freiburg, Department of Radiology, Freiburg, Germany), enable a platform approach, which makes data annotation and postprocessing solutions more accessible, modular, and user-friendly, even across multiple institutions. This has the potential to improve today's workflows, refine clinical-decision making and personalize patient management. As of now, these solutions have been investigated in various research settings to explore their potential role to improve clinical workflows and patient management. The most promising results were found for fully automated organ and tissue segmentation, extraction of quantitative radiomic imaging features, which may facilitate improved tissue characterization and end-to-end deep learning pipelines for individualized risk assessment. However, further research is needed to prove their value in clinical scenarios.

Moreover, since the implementation of more complex and iterative image reconstruction algorithms, the use of traditional image quality metrics such as SNR and CNR for objective image assessment in PCCT remains limited due to the nonlinearity of iterative reconstruction methods [48]. This is also present for different model-based and deep learning reconstructions [49] offered by manufacturers. Further development of new, robust methods will be necessary in the future.

## Conclusion

PCCT has been implemented in the clinical routine and the novel detector technology significantly decreases image noise and artifacts, improves spatial resolution, and reduces radiation dose. In addition, K-edge imaging with material decomposition creates new possibilities for quantitative analyses. To exploit the full potential of PCCT, reliable and automated tools are required to support data analyses and establish efficient and accurate ways for data postprocessing, handling, and storage.

### Conflict of Interest

The authors declare that they have no conflict of interest.

### References

[1] Hounsfield GN. Computerized transverse axial scanning (tomography). 1. Description of system. Br J Radiol 1973; 46 (552): 1016–1022

[2] Ertl-Wagner B et al. [Diagnostic evaluation of the craniocervical vascular system with a 16-slice multi-detector row spiral CT. Protocols and first experiences]. Radiologe 2002; 42 (9): 728–732

[3] Kalender WA. Thin-section three-dimensional spiral CT: is isotropic imaging possible? Radiology 1995; 197 (3): 578–580

[4] Klingenbeck-Regn K et al. Subsecond multi-slice computed tomography: basics and applications. Eur J Radiol 1999; 31 (2): 110–124

[5] Flohr T, Ohnesorge BM et al. Multi-slice CT Technology, in Multi-slice and Dual-source CT in Cardiac Imaging: Principles – Protocols – Indications – Outlook. Berlin, Heidelberg: Springer Berlin Heidelberg; 2007: 41–69

[6] Leng S et al. Spectral performance of a whole-body research photon counting detector CT: quantitative accuracy in derived image sets. Phys Med Biol 2017; 62 (17): 7216–7232

[7] Flohr T et al. Photon-counting CT review. Phys Med 2020; 79: 126–136

[8] Nakamura Y et al. An introduction to photon-counting detector CT (PCD CT) for radiologists. Jpn J Radiol 2022. doi:10.1007/s11604-022-01350-6

[9] Flohr TG et al. Novel ultrahigh resolution data acquisition and image reconstruction for multi-detector row CT. Med Phys 2007; 34 (5): 1712–1723

[10] Leng S et al. Photon-counting Detector CT: System Design and Clinical Applications of an Emerging Technology. Radiographics 2019; 39 (3): 729–743

[11] Rajendran K et al. Full field-of-view, high-resolution, photon-counting detector CT: technical assessment and initial patient experience. Phys Med Biol 2021; 66 (20). doi:10.1088/1361-6560/ac155e

[12] Flohr T et al. Basic principles and clinical potential of photon-counting detector CT. Chinese Journal of Academic Radiology 2020; 3 (1): 19–34

[13] Giersch J, Niederlöhner D, Anton G. The influence of energy weighting on X-ray imaging quality. Nuclear Instruments and Methods in Physics Research Section A: Accelerators, Spectrometers, Detectors and Associated Equipment 2004; 531 (1): 68–74

[14] Persson M et al. Energy-resolved CT imaging with a photon-counting silicon-strip detector. Phys Med Biol 2014; 59 (22): 6709–6727

[15] Shefer E et al. State of the Art of CT Detectors and Sources: A Literature Review. Current Radiology Reports 2013; 1 (1): 76–91

[16] Leng S et al. Dose-efficient ultrahigh-resolution scan mode using a photon counting detector computed tomography system. J Med Imaging (Bellingham) 2016; 3 (4): 043504

[17] da Silva J et al. Resolution characterization of a silicon-based, photon-counting computed tomography prototype capable of patient scanning. J Med Imaging (Bellingham) 2019; 6 (4): 043502

[18] Willemink MJ et al. Photon-counting CT: Technical Principles and Clinical Prospects. Radiology 2018; 289 (2): 293–312

[19] Schlomka JP et al. Experimental feasibility of multi-energy photon-counting K-edge imaging in pre-clinical computed tomography. Phys Med Biol 2008; 53 (15): 4031–4047

[20] Rajendran K et al. High Resolution, Full Field-of-View, Whole Body Photon-Counting Detector CT: System Assessment and Initial Experience. Proc SPIE Int Soc Opt Eng 2021: 11595

[21] Leng S et al. 150-mum Spatial Resolution Using Photon-Counting Detector Computed Tomography Technology: Technical Performance and First Patient Images. Invest Radiol 2018; 53 (11): 655–662

[22] Bartlett DJ et al. High-Resolution Chest Computed Tomography Imaging of the Lungs: Impact of 1024 Matrix Reconstruction and Photon-Counting Detector Computed Tomography. Invest Radiol 2019; 54 (3): 129–137

[23] Grunz JP et al. Image Quality Assessment for Clinical Cadmium Telluride-Based Photon-Counting Computed Tomography Detector in Cadaveric Wrist Imaging. Invest Radiol 2021; 56 (12): 785–790

[24] Si-Mohamed SA et al. Coronary CT Angiography with Photon-counting CT: First-In-Human Results. Radiology 2022; 303 (2): 303–313

[25] Soschynski M et al. High Temporal Resolution Dual-Source Photon-Counting CT for Coronary Artery Disease: Initial Multicenter Clinical Experience. J Clin Med 2022; 11 (20). doi:10.3390/jcm11206003

[26] Virk JS, Singh A, Lingam RK. The role of imaging in the diagnosis and management of otosclerosis. Otol Neurotol 2013; 34 (7): e55–e60

[27] Kanzara T, Virk JS. Diagnostic performance of high resolution computed tomography in otosclerosis. World J Clin Cases 2017; 5 (7): 286–291

[28] Purohit B, Hermans R, Op de Beeck K. Imaging in otosclerosis: A pictorial review. Insights Imaging 2014; 5 (2): 245–252

[29] Duan X et al. Electronic noise in CT detectors: Impact on image noise and artifacts. Am J Roentgenol 2013; 201 (4): W626–W632

[30] Liu Y et al. Reducing image noise in computed tomography (CT) colonography: effect of an integrated circuit CT detector. J Comput Assist Tomogr 2014; 38 (3): 398–403

[31] Iwanczyk JS et al. Photon Counting Energy Dispersive Detector Arrays for X-ray Imaging. IEEE Trans Nucl Sci 2009; 56 (3): 535–542

[32] Yu Z et al. Noise performance of low-dose CT: comparison between an energy integrating detector and a photon counting detector using a whole-body research photon counting CT scanner. J Med Imaging (Bellingham) 2016; 3 (4): 043503

[33] Schmidt TG. CT energy weighting in the presence of scatter and limited energy resolution. Med Phys 2010; 37 (3): 1056–1067

[34] Symons R et al. Low-dose lung cancer screening with photon-counting CT: a feasibility study. Phys Med Biol 2017; 62 (1): 202–213

[35] Long Z et al. Clinical Assessment of Metal Artifact Reduction Methods in Dual-Energy CT Examinations of Instrumented Spines. Am J Roentgenol 2019; 212 (2): 395–401

[36] Schmidt TG. Optimal "image-based" weighting for energy-resolved CT. Med Phys 2009; 36 (7): 3018–3027

[37] Johnson TR et al. Material differentiation by dual energy CT: initial experience. Eur Radiol 2007; 17 (6): 1510–1517

[38] Roessl E, Proksa R. K-edge imaging in x-ray computed tomography using multi-bin photon counting detectors. Phys Med Biol 2007; 52 (15): 4679–4696

[39] Alvarez RE, Macovski A. Energy-selective reconstructions in X-ray computerized tomography. Phys Med Biol 1976; 21 (5): 733–744

[40] Lakshmanan M et al. WE-FG-207B-01: BEST IN PHYSICS (IMAGING): Abdominal CT with Three K-Edge Contrast Materials Using a Whole-Body Photon-Counting Scanner: Initial Results of a Large Animal Experiment. Medical Physics 2016; 43: 3834–3834

[41] Symons R et al. Dual-contrast agent photon-counting computed tomography of the heart: initial experience. Int J Cardiovasc Imaging 2017; 33 (8): 1253–1261

[42] Symons R et al. Photon-counting CT for simultaneous imaging of multiple contrast agents in the abdomen: An in vivo study. Med Phys 2017; 44 (10): 5120–5127

[43] Sartoretti T et al. Photon-counting CT with tungsten as contrast medium: Experimental evidence of vessel lumen and plaque visualization. Atherosclerosis 2020; 310: 11–16

[44] Bornefalk H, Persson M. Theoretical comparison of the iodine quantification accuracy of two spectral CT technologies. IEEE Trans Med Imaging 2014; 33 (2): 556–565

[45] Chen H et al. Optimization of beam quality for photon-counting spectral computed tomography in head imaging: simulation study. J Med Imaging (Bellingham) 2015; 2 (4): 043504

[46] Fedorov A et al. 3D Slicer as an image computing platform for the Quantitative Imaging Network. Magn Reson Imaging 2012; 30 (9): 1323–1341

[47] van Griethuysen JJM et al. Computational Radiomics System to Decode the Radiographic Phenotype. Cancer Res 2017; 77 (21): e104–e107

[48] Vaishnav JY et al. Objective assessment of image quality and dose reduction in CT iterative reconstruction. Med Phys 2014; 41 (7): 071904

[49] Chun M et al. Fully automated image quality evaluation on patient CT: Multi-vendor and multi-reconstruction study. PLoS One 2022; 17 (7): e0271724